Chapter

Pore Formation in Biodegradable Polymers via Supercritical CO_2 Foaming: Mechanisms, Characterization, and Applications

Ignacio García-Casas, Diego Valor, Ludisbel León-Marcos, Antonio Montes and Clara Pereyra

Abstract

The development of porous biodegradable polymers via supercritical CO_2 foaming represents a promising approach towards sustainable materials engineering. This chapter explores the physical and chemical mechanisms behind pore formation in such systems, focusing on gas-polymer interactions, nucleation dynamics, and pore growth during pressure quenching. The process is placed in the context of transport phenomena in porous media, highlighting mass transfer, solubility, and thermodynamic transitions relevant to the foaming process. Recent advances in pore formation are presented, including multiscale approaches that link molecular interactions with macroscopic pore structures. Experimental methods for characterizing the resulting porous architectures—such as Scanning Electron Microscopy (SEM), Mercury Intrusion Porosimetry (MIP), and X-ray Micro-Computed Tomography (μCT)—are discussed to assess porosity, pore size distribution, and interconnectivity. The chapter also examines how the structure-property relationships of these foamed biodegradable polymers can be optimized for practical applications in biomedical devices, packaging, and filtration systems. Emphasis is placed on the environmental benefits of using CO_2 as a green blowing agent and biodegradable polymers as a renewable substrate. This paper aims to bridge fundamental understanding and real-world applicability, in line with current theoretical advances and future opportunities in porous media research.

Keywords: $scCO_2$ foaming, biopolymers, porous materials, morphology, scaffolds

1. Introduction

The widespread use of conventional plastics has generated growing environmental concern due to their long degradation times and their tendency to accumulate in terrestrial and marine ecosystems. In response, biodegradable polymers have emerged

as a promising alternative. These materials can naturally degrade through microbial activity, breaking down into harmless by-products, such as carbon dioxide, water, and biomass. This makes them key components in the transition towards a circular economy based on sustainable materials.

Biodegradable polymers can be classified by origin as natural (e.g., starch, cellulose, and proteins), semi-synthetic or synthetic (e.g., PLA (polylactic acid), PBS (poly(butylene succinate)), and PBAT (poly(butylene adipate-co-terephthalate)) [1]. They have a wide range of applications, including packaging, agriculture, biomedicine, and other environmentally sensitive areas where recyclability is not an option or where contact with living tissues or food requires safety and purity [1, 2].

Despite their environmental advantages, biodegradable polymers often present processing challenges, such as low thermal stability, limited melt strength, or crystallization kinetics, which complicate the fabrication of advanced materials. In this context, polymer foaming has emerged as a technique that can enhance properties while reducing material usage. Foaming introduces a cellular structure into the polymer matrix, resulting in lightweight materials with improved thermal, acoustic, and mechanical properties that are useful in packaging, insulation, filtration, and the biomedical field [1].

Foaming techniques are usually categorized as chemical, mechanical, or physical. Chemical foaming uses blowing agents that thermally decompose to release gas and form cells. However, they often leave behind residual chemicals, which make them less suitable for sensitive applications [3, 4]. Mechanical foaming involves injecting gas through agitation, but this method offers limited control over the final morphology. In contrast, physical foaming with supercritical CO_2 ($scCO_2$) provides precise control over the structure and avoids the use of toxic solvents [4].

The $scCO_2$ foaming process involves two main stages: (i) saturation, in which CO_2 diffuses into the polymer at an elevated pressure and temperature; and (ii) depressurization, which causes a sudden drop in solubility and leads to the nucleation and growth of gas bubbles [2, 5]. The structure of the resulting foam (cell size, density, and uniformity) is strongly influenced by parameters, such as saturation pressure and temperature, time, and depressurization rate [6, 7]. A key feature of $scCO_2$ is its plasticizing effect, which reduces the glass transition temperature (Tg) and viscosity of polymers, enabling processing at lower temperatures—critical for thermally sensitive biodegradable polymers, such as polylactic acid (PLA) and thermoplastic starch (TPS) [1, 8].

Furthermore, $scCO_2$ is non-toxic, inert, and non-flammable, and it does not leave behind any harmful residues, making it ideal for use in food packaging and biomedical devices [1, 2]. In addition to enabling structural control, $scCO_2$ allows functional additives (e.g., drugs, antioxidants, and antimicrobials) to be impregnated simultaneously during foaming, facilitating the production of multifunctional porous materials [1]. For example, active packaging materials or drug-loaded scaffolds for tissue engineering can be produced in a single step using supercritical CO_2.

The foaming efficiency of a polymer depends on its molecular characteristics. PLA, for example, is widely used, but it has low melt strength, which can cause bubbles to collapse [9]. Starch-based polymers, on the other hand, are difficult to foam due to their hydrophilicity and weak mechanical properties [7]. To overcome these issues, researchers have investigated the use of polymer blends, chain extenders, and nanoparticle fillers, such as calcium carbonate ($CaCO_3$) or carbon nanofibers, to improve foam stability, nucleation, and mechanical performance [10, 11].

In summary, $scCO_2$ foaming of biodegradable polymers is a versatile, sustainable, and high-performance method of producing advanced porous materials, with increasing potential in industries that demand environmentally responsible solutions.

2. Supercritical carbon dioxide: A smart tool for clean polymer processing

Supercritical carbon dioxide is a fluid that becomes supercritical when the temperature exceeds 31.1°C and the pressure exceeds 7.38 MPa [4, 8]. Under these conditions, it exhibits a unique combination of liquid-like density and gas-like diffusivity, enabling efficient dissolution, swelling, and penetration of polymer matrices—making it an ideal medium for polymer processing and foaming [4].

In polymer foaming, $scCO_2$ acts as a physical blowing agent, plasticizing the polymer and reducing its viscosity and glass transition temperature (Tg) [8]. This enables thermally sensitive biodegradable polymers, such as PLA and starch derivatives, to be processed without compromising their integrity [1]. Its non-toxic, inert, and solvent-free nature also makes it ideal for use in biomedicine and food packaging [2].

A key advantage of supercritical carbon dioxide ($scCO_2$) is that its solvent power can be tuned by adjusting the pressure and temperature. This provides precise control over gas solubility, nucleation, and foam cell morphology, enabling micro- or nanocellular structures to be created that are optimized for specific functions ranging from thermal insulation to biomedical scaffolds [4, 5]. Furthermore, $scCO_2$ can impregnate functional molecules into the polymer matrix during foaming, expanding its use in producing active materials for drug delivery or antimicrobial packaging [1].

Although the potential of $scCO_2$ foaming is promising, its industrial-scale implementation still faces challenges, including the cost of high-pressure equipment, the need to optimize the process for each polymer, and scaling limitations [2]. Nevertheless, advancements in CO_2-assisted extrusion, gas co-blowing strategies, and eco-efficient process design are being actively pursued [6, 7]. Overall, $scCO_2$ offers a clean, tunable, and efficient approach to producing biodegradable foam, in line with the principles of green chemistry and modern goals for sustainable manufacturing.

In addition to its technical advantages, $scCO_2$ foaming offers significant environmental benefits. Unlike conventional chemical blowing agents, which may release volatile organic compounds (VOCs) or leave residues, $scCO_2$ is non-toxic, recyclable, and leaves no residue. It enables solvent-free processing and eliminates the need for post-treatment purification, thereby reducing energy and material consumption. From a sustainability perspective, the CO_2 used in foaming can be captured from industrial emissions, transforming waste gas into a valuable resource—a process known as carbon capture and utilization (CCU). Furthermore, most industrial systems operate in closed loops, enabling repeated CO_2 recovery with minimal losses and low environmental impact. While maintaining supercritical conditions does require energy, this is often offset by the lower processing temperatures enabled by the plasticizing effect of $scCO_2$. This reduces degradation and energy input compared to thermal or solvent-based foaming methods.

Comparative studies show that when biodegradable or bio-based polymers are used, supercritical CO_2 foaming achieves one of the lowest environmental footprints among current foaming technologies. The resulting materials are compatible with circular economy models, particularly when polymers such as PLA, poly(ε-caprolactone) (PCL), or starch derivatives are used.

3. Biodegradable polymers

This section provides a comprehensive overview of biodegradable polymers, focusing on their definition, classification, and specific types relevant to foam formation using supercritical carbon dioxide ($scCO_2$). Particular attention is paid to the physicochemical properties that determine their suitability for this advanced processing technique, especially thermal transitions and interactions with $scCO_2$.

3.1 Fundamental concepts and terminology

A biodegradable polymer is defined as a polymeric material that degrades as a result of the metabolic activity of microorganisms, such as bacteria, fungi, or algae [12]. This biodegradation process leads to the formation of biomass and carbon dioxide (CO_2) under aerobic conditions or methane (CH_4) under anaerobic conditions, as well as water and mineral salts [12]. This definition highlights the biological mechanism as the main cause of degradation, setting it apart from other degradation pathways, such as photodegradation or oxidative degradation, which do not necessarily involve microbial assimilation or the complete mineralization of substances into harmless end products.

The environmental context and temporal framework are crucial aspects of this definition. Ideally, biodegradable materials should decompose within a reasonable timeframe (e.g., within a year) in the most common disposal environment, transforming into non-toxic end products, such as humus, water, or CO_2. However, 'biodegradability' is not an absolute material property, but rather one that depends heavily on specific environmental conditions and time. For example, although polylactic acid (PLA) is compostable under industrial conditions (55–60°C), it may not readily degrade in natural environments such as the ocean or soil, where it may instead fragment into microplastics. Degradation rates are critically influenced by environmental factors, such as temperature, pH, and oxygen availability, as well as polymer formulation [13].

It is important to distinguish between 'biodegradable' and 'degradable' polymers. The latter may decompose via non-biological mechanisms, meaning they are not necessarily microbially assimilated or mineralized. The term 'bioplastics' is also frequently used and can refer to bio-based materials from renewable sources, biodegradable materials, or both [12].

3.2 Overview of biodegradation mechanisms

Biodegradation of polymers is a multiphase process that usually starts with biofragmentation. In this stage, polymer chains are broken down into smaller oligomers and monomers by extracellular enzymes released by microorganisms, or through initial abiotic processes that facilitate microbial access. These low-molecular-weight fragments can then be taken up by microbial cells and metabolized.

A polymer's susceptibility to biodegradation is influenced by multiple factors. The chemical structure is paramount in dictating the stability of functional groups, reactivity (especially towards enzymatic hydrolysis), hydrophilicity, and water-swelling behavior, which facilitates microbial attack. Other intrinsic factors include crystallinity (amorphous regions are generally more degradable), molecular weight (shorter chains degrade faster), and morphology. Environmental conditions, such as temperature, humidity, pH, and microbial population composition, are also critical [12].

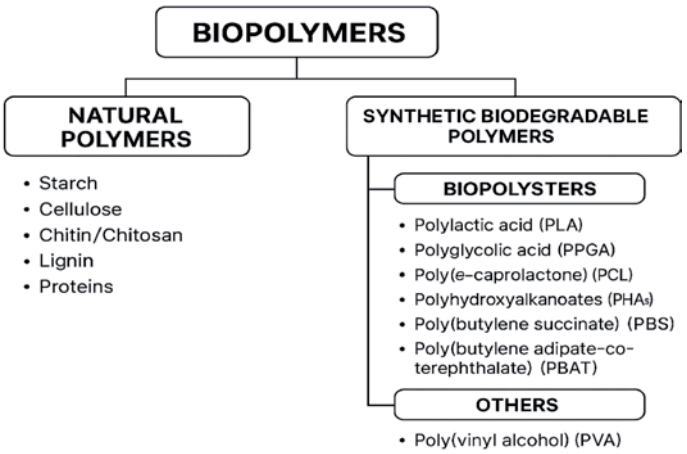

Figure 1.
Scheme of polymers according to their source.

3.3 Classification and types of biodegradable polymers

Biodegradable polymers exhibit considerable diversity. They originate from various sources and their distinct chemical structures determine how they degrade and can be processed (**Figure 1**).

Natural Polymers: Derived directly from biomass including plants, animals, or microbial sources. These polymers are inherently biodegradable and renewable but often require modification to meet processing and performance criteria for foam applications.

Synthetic Biodegradable Polymers: These are chemically synthesized from either bio-based monomers or fossil-derived precursors. Their biodegradability is engineered into the polymer backbone, often through hydrolysable linkages. They offer tailored properties and controlled degradation rates, making them highly relevant to advanced applications such as scCO2 foaming.

A trade-off exists between source and processability. While natural polymers like starch and cellulose are abundant and renewable, they typically require significant chemical modification (e.g., starch to TPS [14], cellulose to cellulose acetate (CA) [15]) to become thermoplastic and amenable to melt-based foam processing such as $scCO_2$ extrusion. In contrast, synthetic biopolyesters like PLA, PCL, or polyhydroxyalkanoates (PHAs) are often designed for better processability, even though they present challenges such as low melt strength (e.g., PLA). Hence, there is often a balance between the sustainability of raw materials and their direct applicability to advanced processing. Life-cycle considerations, including energy input and chemical modification steps, are essential in assessing the overall sustainability of $scCO_2$-foamed biodegradable products.

4. Supercritical foaming process

The supercritical foaming process is a process that uses supercritical fluid, commonly CO_2, to generate a porous and interconnected structure in a polymer. The polymer foaming process generally involves three core stages: the creation of a

homogeneous polymer/gas system, the nucleation of cells, and the subsequent growth and stabilization of these cells. In this process, CO_2 is brought into contact with the polymer to be treated under supercritical conditions. As can be seen in the diagram in **Figure 2**, the CO_2 is pumped to the chosen operating conditions (pressure and temperature) inside the chamber where the polymer is located.

The operating temperature must generally be above the glass transition temperature (Tg) for amorphous polymers and above the melting temperature (Tm) for crystalline polymers. This is why amorphous polymers or those with a large amorphous domain are generally used, so that the operating temperature is not too high.

The polymer and CO_2 must be able to form a solution where the CO_2 needs to diffuse to carry out the nucleation and growth process of the bubbles. The gas's plasticizing effect on the polymer increases the mobility of the polymer molecular chains, which in turn lowers the free energy barrier for cell nucleation. This cell nucleation is driven by thermodynamic instability within the system. Once a contact time has elapsed, the chamber is subjected to controlled depressurization using a micrometric depressurization valve, causing the dissolved CO_2 to lose its solubility in the polymer. This reduction in CO_2 solubility could also be achieved by increasing the temperature in the chamber.

The supersaturation of the gas (**Figure 3**) within the polymer causes the nucleation of millions of small bubbles (cells). The uniformity and size of these cells are fundamental for the properties of the final product. In this sense, higher saturation pressure and a lower temperature, a priori, favor the formation of smaller and more homogeneous cells. The newly formed bubbles grow as the gas expands. However, only nuclei that attain a critical size can maintain stability. Subsequently, the gas dissolved within the polymer matrix diffuses into the cell nucleus, leading to an increase in its diameter. The viscosity of the polymer and surface tension play an important role in this growth. Precise control of the temperature and decompression rate during this stage is vital to obtain the desired density, cell size, and porous structure of the final porous structure.

This process can be modified by including additives and/or pore generators to achieve greater nucleation and interconnection of the formed pores. The most

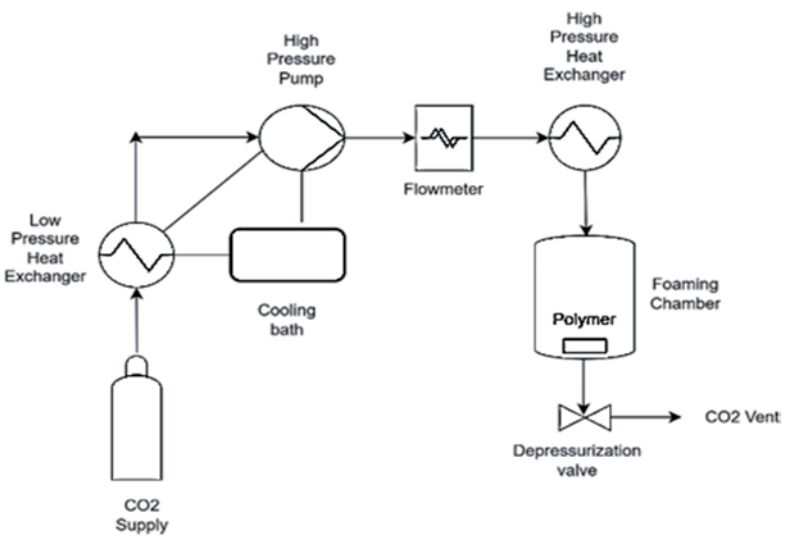

Figure 2.
Supercritical foaming process pilot plant.

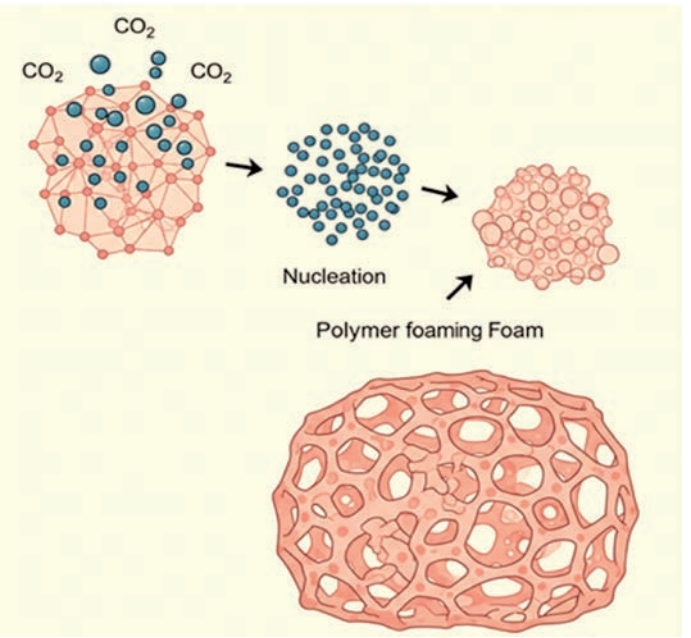

Figure 3.
Supercritical foaming process scheme.

widespread approach is to use inorganic particles to promote heterogeneous nucleation. These particles provide specific sites in the polymer matrix where the supercritical gas can nucleate more easily when pressure is reduced or temperature is increased. By having a surface with high interfacial energy with the polymer and the gas, they act as seeds for bubble formation. Some examples of particles used are silica nanoparticles [16], titanium dioxide [17], calcium carbonate [18], glass or carbon fibers [19], clays [20], which even improve mechanical properties, or carbon nanotubes [21], which can improve the mechanical, electrical, and thermal properties of the formed polymers. The pore generation effect could also be achieved by adding another polymer with a different glass transition or melting temperature to create heterogeneity in the matrix that favors nucleation, since when one of the polymers reaches its Tg or Tm and the other does not, interfacial stresses are generated that can promote bubble nucleation.

4.1 Process optimization strategies and control tools

Optimizing supercritical CO_2 ($scCO_2$) foaming conditions requires balancing thermodynamics, gas solubility, polymer rheology, and kinetics. The key variables—pressure, temperature, saturation time, and depressurization rate—must be tailored to each polymer system to achieve desired pore structure, porosity, and interconnectivity. **Table 1** summarizes optimal ranges of pressure and temperature for three commonly used biodegradable polymers.

4.2 Guidelines for parameter selection

A simplified decision guide (**Figure 4**) is provided to assist in parameter selection:

Polymer	Optimal Pressure (bar)	Optimal Temperature (°C)	Notes
PLA	150–250	35–45	Lower temperatures preserve polymer integrity; high pressure improves cell density
PCL	100–200	40–70	Broader range due to flexibility; higher T favors expansion but risks collapse
PBS	120–160	100–115	Typically foamed near melting point; blends enhance open-cell structure

Table 1.
Optimal ranges of pressure and temperature.

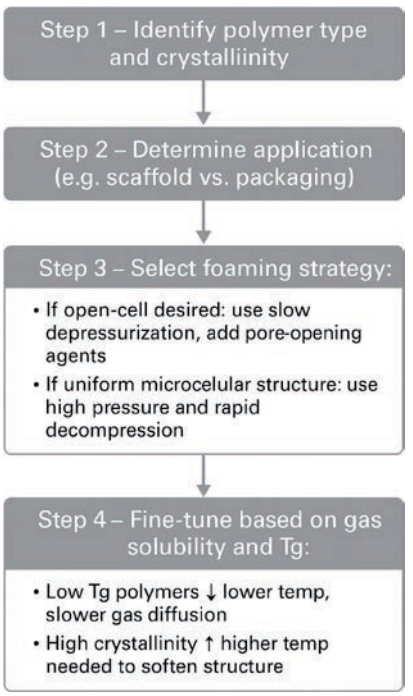

Figure 4.
Parameter selection decision guide.

5. Mechanisms

The processes implied in supercritical foaming are divided into several steps. First, a solution of gas/polymer should be formed. Then, the diffusion and nucleation of bubbles of gas into the polymer structure occur. This nucleation can be homogeneous or heterogeneous, depending on the presence or absence of inorganic particles within the polymer. The subsequent steps include growing, stabilization, and pore formation.

5.1 Gas/polymer solution formation

The process starts when a blowing agent, typically carbon dioxide (CO_2), is introduced into the polymer. Under high pressure, the CO_2 gas directly dissolves

into the polymer melt without any chemical reaction. This creates a uniform polymer/gas solution. The more gas that dissolves, the lower the final foam density will be. Factors like temperature, pressure, and the specific chemical attraction between the gas and the polymer all influence how much gas dissolves. Interestingly, the dissolved CO_2 acts as a plasticizer for the polymer. This means it significantly reduces the polymer's melt viscosity and lowers its glass transition temperature (Tg). This plasticizing effect is crucial because it makes it easier for the gas to move around and for bubbles to grow [22].

5.2 Cell formation

Once the polymer-gas solution is formed, a thermodynamic instability is introduced, usually by rapidly dropping the pressure or increasing the temperature. This makes the dissolved gas supersaturated within the polymer [1]. When the solution becomes supersaturated, the gas wants to escape and clump together, forming tiny gas bubbles called cell nuclei. This process is called nucleation. If the supersaturation is high enough, these nuclei can form spontaneously throughout the solution (this is called homogeneous nucleation). However, if there are particles or impurities in the system, they act as preferred spots for bubble formation, as they lower the energy barrier for nucleation. This is known as heterogeneous nucleation, and it often leads to a more uniform cell structure [23].

Once nuclei are formed, dissolved gas from the surrounding polymer quickly diffuses into these growing bubbles. The main reason why this happens is the difference in gas concentration. The higher the gas diffusivity, the faster the bubbles will grow [22]. The pressure of the gas inside a growing cell is inversely related to its radius, this means smaller bubbles have higher internal pressure. As a result, gas tends to move from areas of higher pressure (smaller bubbles) to areas of lower pressure (larger bubbles). This causes smaller bubbles to shrink and disappear while larger ones continue to grow.

The viscoelastic properties of the polymer melt are also critical for controlling cell growth. The polymer needs enough melt strength to resist the outward pressure from the expanding bubbles, which prevents the bubbles from merging prematurely or rupturing. At the same time, it needs to be fluid enough to allow gas to diffuse and the bubbles to expand.

5.3 Cell stabilization

The inherent melt strength of the polymer is a key point for stabilizing the cellular structure. Polymers with higher melt strength are better at holding onto the cellular structure and preventing cells from merging, especially during the growth phase. One common way to stabilize the foam is by rapid cooling [10]. As the temperature drops, the polymer's viscosity increases dramatically, essentially 'freezing' the bubbles in place and preventing them from growing further or collapsing. Alternatively, stabilizing agents like surfactants, specific polymers, or fillers can be added to the polymer solution. These agents increase the viscosity of the cell walls, making them more resistant to drainage and rupture. In some cases, such as with thermoset foams like polyurethane, chemical crosslinking reactions occur during foaming, which creates a rigid network that permanently stabilizes the cellular structure.

6. Comprehensive analysis of foam morphologies and properties of key biodegradable polymers

6.1 Poly(lactic acid) (PLA) and copolymers (PLGA, PLLA)

Poly(lactic acid) (PLA) and its derivatives, such as poly(L-lactic acid) (PLLA) and poly(lactic-co-glycolic acid) (PLGA), are widely studied biodegradable polymers, primarily due to their predictable resorption rates and well-documented biocompatibility[1]. These polymers have been instrumental in the development of porous scaffolds for tissue engineering, particularly when processed with supercritical carbon dioxide ($scCO_2$).

6.1.1 Porosity, pore size, and connectivity characteristics

Scaffolds based on PLA and its copolymers typically achieve high porosity values, with multiple reports citing void fractions above 80%. For instance, PLGA-based foams have been shown to achieve porosity levels of up to 94.97% [24], while PLA/PBS blends have demonstrated values as high as 97.7% [25]. Levels of this kind have been recorded in poly(DL-lactide) (P(DL)LA) and poly(DL-lactide-co-glycolide) (P(DL)LGA) systems [26], thus highlighting the suitability of $scCO_2$ processing for the generation of low-density, high-surface-area matrices.

The average pore size in these foams varies significantly depending on both material formulation and processing parameters. For instance, PLGA scaffolds typically exhibit pores with a diameter ranging from 30 to 200 μm, which are conducive to supporting diverse cell types. The addition of chitosan has been demonstrated to result in a reduction of pore size from 190 to 110 μm [27]. The incorporation of magnetic nanoparticles (SPIONs (superparamagnetic iron oxide nanoparticles)) has also been demonstrated to contribute to pore size refinement [24]. In neat PLA, mean pore diameters of approximately 109 μm can be reduced to ~21 μm through the addition of 3 wt% microcellulose fibrils [28]. Ternary blends such as PLA/PBS/PBAT frequently exhibit bimodal pore architectures, with distinct populations of small pores (105–164 μm) and larger macropores (476–889 μm) [29].

Pore interconnectivity is another critical parameter for tissue scaffolds, influencing nutrient diffusion and cell migration. This feature can be significantly enhanced by means of formulation adjustments and precise control of processing conditions [30]. For instance, silica-reinforced PLGA foams exhibit increased network continuity [31], while the addition of chitosan enhances pore interconnections by up to 2.5 times [27]. Blends of PLA/PBS yield highly open structures, with up to 98.2% open cells [25]. The rate of depressurization is also of pivotal significance. Slower rates have been observed to promote pore coalescence and network connectivity, while rapid decompression has been shown to favor smaller and more isolated pores [30].

6.1.2 Effects of processing parameters

Increased pressure during the process of $scCO_2$ foaming has been shown to reduce average pore size; this trend has been observed to be consistent across a variety of systems, with enhanced homogeneity and finer pore distributions being noted at pressures greater than 250 bar [32]. In composite systems such as PLGA/SPIONs, pressure is a pivotal factor in achieving multimodal morphologies [24].

Temperature exhibits a significant influence on both the rate of diffusion of CO_2 and the viscosity of the polymer melt. It has been established that moderate increases in temperature result in the dilatation of pores, while very high temperatures can cause structural collapse due to a reduction in melt strength [33]. However, PLA/PBS/PBAT blends demonstrate an inversion of this trend, with elevated temperatures resulting in diminished pore size. This phenomenon may be attributed to alterations in gas solubility and melt rheology [34]. In the case of more sensitive copolymers such as P(3HB-co-4HB) (poly(3-hydroxybutyrate-co-4-hydroxybutyrate)), lower processing temperatures are required as the proportion of 4-hydroxybutyrate (4HB) increases [35].

Brief periods of saturation may result in the formation of heterogeneous structures, characterized by a dense core and a porous shell. Optimal times (e.g., 10 minutes) have been shown to enhance porosity and average pore size, while prolonged saturation has been observed to decrease pore dimensions by promoting overplasticization [30]. In PLGA-based systems, the application of extended durations of up to 2 hours has been shown to result in the achievement of consistent foaming behavior [36]. Gradual depressurization has been shown to promote interconnectivity and wider pore distributions [30]. Conversely, rapid decompression has been shown to promote homogeneity and smaller pore size, but may increase closed-cell content. In PLGA/SPION systems, it is imperative to meticulously modulate this rate to yield hierarchically and functionally graded pore networks. Nevertheless, it has been demonstrated that a sluggish process of depressurization may impede the process of foam expansion, should gas effusions occur prior to the stabilization of pores [36].

6.1.3 Effect of additives and polymer blends

The blending of PLA with TPU (Thermoplastic Polyurethane) in solvent-free $scCO_2$ processes has been shown to result in the production of foams that exhibit enhanced elasticity and increased open-cell content. Foams containing 50% TPU achieved open porosity levels of up to 96.2%, while blends comprising 30% TPU demonstrated a high expansion ratio of 36.06. Furthermore, TPU has been demonstrated to enhance PLA crystallinity, thereby contributing to enhanced foam stability.

PLA with PBS (poly(butylene succinate)) blends are distinguished by their full biodegradability and highly interconnected structures. The materials demonstrate porosity levels of up to 97.7%, accompanied by 98.2% open-cell content, thus substantiating their efficacy in filtration and environmental applications [25]. Furthermore, PBS has been demonstrated to contribute to morphological tuning, favoring open-cell formation.

PLA/PBS with PBAT (poly(butylene adipate-co-terephthalate)) ternary systems, when reinforced with nanohydroxyapatite (nHA), exhibit a wide porosity range (26.5–94.4%) and diverse open-cell contents (12.7–84.3%), depending on the process conditions to which they are subjected [29]. The presence of bimodal pore populations enhances their suitability for tissue engineering.

PLA with MCFs (Microcellulose Fibrils) functions as a potent nucleating agent, resulting in a substantial reduction in average pore size, from 109 to 21 μm [28]. It has been demonstrated that open porosity increases with low MCF loading (from 71.8 to 76.1% with 1.5% MCF), but may decrease at higher concentrations. This indicates an upper limit beyond which excessive filler impairs porosity.

The incorporation of chitosan has been shown to result in a reduction of the average pore size, accompanied by a substantial enhancement in pore interconnectivity

[27]. However, it is noteworthy that elevated levels of chitosan or the incorporation of phytochemical extracts (e.g., derived from olive pruning) have been observed to impede the formation of fine pores and thereby reduce overall porosity.

The integration of conductive polymers, such as PEDOT:PSS (poly(3,4-ethylenedioxythiophene):polystyrene sulphonate), into PLGA facilitates the fabrication of electroactive scaffolds. These materials exhibit moderate porosity (approximately 40%) alongside electrical conductivities ranging from 2.2×10^{-7} to 1.0×10^{-5} S/cm [37]. The uniform distribution of PEDOT:PSS is conducive to both structural integrity and electrical continuity, rendering these scaffolds promising candidates for neural or cardiac regeneration.

6.2 Poly(ε-caprolactone) (PCL) and composite systems

Poly(ε-caprolactone) is a semicrystalline aliphatic polyester that has gained a reputation for its biodegradability, biocompatibility, and mechanical flexibility, which render it highly suitable for tissue engineering applications [38]. Its relatively low melting point and ease of processing render it compatible with supercritical CO_2 ($scCO_2$) foaming methods.

6.2.1 Porosity, pore size, and connectivity characteristics

Porosity values of up to 89% have been documented in the literature [5], and interconnectivity can attain 96% in certain low-molecular-weight PCL systems (e.g., 27 kDA) [39]. While the incorporation of nanofillers generally results in porosity levels above 80% [38], the inclusion of bulky porogens or ceramic fillers has been observed to reduce porosity due to space competition. For instance, in PCL/HA (hydroxyapatite) composites, porosity typically ranges from 65.6 to 74.4% at 40°C and from 61.9 to 67.1% at 50°C [40]. Analogous trends have been observed in scaffolds impregnated with carvacrol [40].

The mean pore diameter of pure PCL foams is typically found to be within the range of 70–180 μm [39]. However, it is important to note that this range can be significantly altered in the processing stage. For instance, an increase in saturation pressure from 100 to 200 bar (at 40°C) has been shown to result in a reduction of the average pore size from 622 ± 62 to 85 ± 24 μm [33]. PCL/HA composites exhibit smaller pores, attributable to the nucleating effect of HA, with a typical range of 40–250 μm [29]. It is interesting to note that, following impregnation with carvacrol, there was a slight increase in pore size, from 133 to 140 μm [40]. The PCL/nC (nanocellulose) and PCL/nGO (graphene oxide) systems demonstrate notable nucleation behavior. These additives typically result in d10 values under 30 μm, although maximum pore sizes of up to 150 μm have been reported for low nGO loadings (0.2 wt%) [38].

Foams from 27 kDa PCL have been shown to reach interconnectivity values of 96% [39]. The incorporation of modest quantities of ethanol during the $scCO_2$ processing phase has been demonstrated to encourage the formation of more open and uniform pore structures, thereby enhancing the morphology relative to that of neat CO_2 [30]. The utilization of plasticizers, such as eugenol, has been demonstrated to promote enhanced throat connectivity and mesenchymal stem cell migration [41]. The employment of advanced processing methodologies, such as two-step depressurization, has resulted in the generation of bimodal, highly interconnected scaffolds, which are highly conducive to applications in regenerative medicine [40].

6.2.2 Effects of processing parameters

An increase in pressure from 100 to 200 bar at 40°C has been shown to result in a reduction in average pore size of almost sevenfold [33]. Moderate increases in temperature have been shown to enhance CO_2 diffusion and reduce melt viscosity, thereby promoting pore expansion [30]. However, at elevated temperatures, structural instability can lead to the formation of collapsed or dense morphologies [39]. In the context of PCL/HA foams, an increase in temperature from 40 to 50°C has been observed to result in a narrowing of the pore size distribution. However, this increase in temperature can also lead to phase coalescence and morphological irregularities [40]. In the context of biomedical scaffolds, a frequently cited compromise between structure and integrity is 70°C [38].

For PCL, durations ranging from seconds to one hour have been the subject of exploration [29]. It has been demonstrated that an increase in duration (e.g., 1 hour) generally results in larger pores and enhanced interconnectivity [38]. It has been demonstrated that rapid decompression (e.g., 20 mmHg/min) results in the uniformization of cell sizes throughout the matrix [38]. It has been demonstrated that a reduction in the rate of depressurization allows for a greater duration in which cell growth and coalescence can occur, thus resulting in the formation of larger, more interconnected pores [30]. Multistep depressurization strategies, including two-step release, have been shown to be especially effective for generating bimodal, interconnected architectures [40].

6.2.3 Effect of additives and composite design

PCL/HA (hydroxyapatite). It has been demonstrated that both micro- and nano-sized HA function as effective nucleating agents, promoting the formation of smaller pores and increasing their density [38]. The porosities of these composites are typically found to be within the range of 55–85%, with pore sizes varying from 40 to 250 μm [29]. While HA strengthens the structure by integrating into pore walls, micro-HA (μHA) has been observed to produce more heterogeneous morphologies than nano-HA (nHA) [38].

PCL/PANI (polyaniline). The incorporation of polyaniline (PANI) into the composition of the material results in the introduction of electrical conductivity while maintaining the integrity of the foam architecture. Despite the absence of direct foaming, PANI domains are uniformly dispersed within the PCL matrix. The resulting scaffolds demonstrate porosities of approximately 50%, and conductivities that are well suited for bioelectronic applications [42].

6.3 Polyhydroxyalkanoates (PHAs), including PHBV

PHAs and PHBV (poly(3-hydroxybutyrate-co-3-hydroxyvalerate)) are microbial-synthesized biodegradable polymers that provide an eco-friendly alternative to fossil-based plastics [35].

6.3.1 Porosity, pore size, and connectivity characteristics

The porosity levels of PHA foams are found to be contingent on both formulation and processing parameters. In particular, PHBV foams have been found to form open-cell structures with notably high porosity [43]. However, the foaming behavior of PHBV can be restricted due to the limited solubility of CO_2 in the polymer matrix [44].

The dimensions of pores in PHAs can be tuned by modifying the conditions under which they are processed. The average cell area of PHBV foams has been shown to be approximately 116.6 μm^2 [43], and earlier reports have achieved pore diameters ranging from 6 to 22 μm in microcellular structures [44]. In the context of P(3HB-co-4HB), it has been observed that elevated foaming pressures are associated with the formation of larger cells [35].

The degree of interconnectivity exhibited by PHA foams is subject to variation. PHBV has the capacity to develop open-cell morphologies that permit a certain degree of connectivity, which renders it a promising material for biomedical applications [43]. However, the formation of well-interconnected pore networks may be hindered by the material's mechanical rigidity [43].

6.3.2 Effects of processing parameters

The application of elevated foaming pressure has been demonstrated to enhance CO_2 uptake and nucleation density, thereby increasing cell population [45]. Furthermore, elevated pressures have been shown to result in larger cell diameters and higher expansion ratios [35].

The ideal foaming temperature is contingent upon the 4HB ratio and the degree of crystallinity. For instance, P(3HB-co-10% 4HB), with higher crystallinity, forms cell structures around 130°C, while more amorphous versions (e.g., P(3HB-co-30% 4HB)) foam effectively between 50 and 80°C [35]. The utilization of chain extenders has been employed to extend this temperature window [45].

For P(3HB-co-4HB), a 60-minute saturation time followed by rapid depressurization to atmospheric pressure has been applied [35]. It is evident that these variables play a pivotal role in shaping the pore structure, although the precise nature of their influence remains to be elucidated.

6.4 Poly(butylene succinate) (PBS) and blends

Poly(butylene succinate) (PBS) is a biodegradable aliphatic polyester that is frequently blended with other polymers to enhance foam morphology, particularly open-cell formation [25].

6.4.1 Porosity, pore size, and connectivity characteristics

Poly(butylene succinate) (PBS)-based foams, particularly those in blend form, have the capacity to attain notably elevated levels of porosity. For instance, the porosity levels of PLA/PBS foams have been reported to reach as high as 97.7% [25]. Pure PBS foam is generally categorized as microcellular, although precise porosity data are not always provided [43].

Foams composed of neat PBS exhibited an average pore area of 673 μm^2 [43]. In composite blends such as PLA/PBS/PBAT, dual-size cellular networks are frequently reported, with smaller pores measuring between 105 and164 μm and larger ones between 476 and 889 μm [29]. PBS foams reinforced with cellulose nanocrystals also exhibit bimodal structures, with larger pores measuring approximately 68.9 μm and smaller ones measuring approximately 11.0 μm [25].

PBS is a structural modifier that has been extensively utilized to enhance pore openness. Typically, PLA/PBS foams develop a highly interconnected, lace-like structure with up to 98.2% open-cell content [9]. PLA/PBS/PBAT systems have

been shown to achieve up to 84.3% open cells under optimized foaming conditions [44]. In contrast, pure PBS has been observed to form predominantly closed cells with thin walls [43].

6.4.2 Effects of processing parameters

Foaming of PBS is commonly conducted at its melting point (113°C) [43]. In blends that contain PBS, intermediate foaming temperatures have been shown to have a significant effect on macropore formation. A reduction in foaming temperature to approximately 100°C in PLA/PBS/PBAT blends has been shown to result in the formation of larger pores (889.8 ± 66.2 μm) and higher open-cell fractions [34].

Pure PBS foaming was carried out at 15 MPa [43]. In blends, a decrease in intermediate pressure drop (from 120 to 80 bar) has been linked with increased cell size and porosity [34], which is consistent with classical nucleation theory, where greater pressure drops facilitate cell expansion.

PBS foams were subjected to a CO_2 saturation time of 30 minutes [43], while PBS/PBAT blends were equilibrated over 90 minutes to ensure complete gas absorption [34].

For neat PBS, the process of depressurization was initiated rapidly (within 2–4 seconds) [43]. Conversely, the utilization of blended systems has been shown to be advantageous due to the stepwise depressurization process, which has been demonstrated to yield bimodal cell structures and enhanced interconnectivity [29].

The incorporation of PBS into PLA has been demonstrated to promote the development of highly interconnected cell architectures [25]. The incorporation of nanoparticles, such as nanohydroxyapatite (nHA), into ternary systems comprising PLA/PBS/PBAT has been demonstrated to enhance hydrophilicity and mechanical performance [34].

6.5 Cellulose and chitosan/derivative-based polymers

Cellulose and chitosan are two naturally abundant biopolymers with promising characteristics for supercritical CO_2 ($scCO_2$) foaming. The inherent hydrophilicity, biocompatibility, and renewable nature of these materials render them particularly well suited to applications, such as biomedical scaffolds and the fabrication of porous materials with large surface areas [2].

6.5.1 Porosity, pore size, and connectivity characteristics

The production of cellulose-based aerogels via scCO2 drying processes has been shown to result in the attainment of remarkably elevated levels of porosity, frequently ranging from 80 to 99.9% [46]. For instance, nanocrystalline cellulose (NCC) aerogels demonstrate porosities ranging from 91 to 95%, while ionic-liquid-treated pulp subjected to scCO2 drying reaches approximately 94–96% [46]. Furthermore, microcrystalline cellulose (MCC) processed under analogous conditions has been shown to exhibit porosities of 91–96% [46].

Chitosan scaffolds exhibit a wide range of porosities, commonly reported between 88 and 97 or 75 and 85% when interconnected pore networks are formed [47]. However, the available quantitative data on the foaming of chitosan solely by $scCO_2$ are limited; the majority of findings relate to structures formed through supercritical drying or gelation [47].

Pore dimensions vary considerably depending on the cellulose form and process. In $scCO_2$-dried aerogels, fibrils are typically characterized by a diameter of approximately 40 nm, while mesh distances can extend over several hundred nanometers [46]. Cellulose cryogels have demonstrated an enhancement in average pore size, ranging from 4.3 to 7.5 μm. In foamed cellulose acetate, the range of pore diameters is from 80 to 20 μm, with pressure being a key factor in size reduction [48].

The utilization of supercritical carbon dioxide ($scCO_2$) during the drying process of aerogels typically results in the preservation of their porous networks, which are characterized by significant interconnectedness. This phenomenon can be attributed to the elimination of capillary forces during the drying process, a process that has been shown to help retain the original gel structure and avoid pore collapse [46].

Interconnected architectures are commonly achieved in architectures derived from chitosan, with descriptions including 'polygonal and interconnected pores' or 'spherical pores in communication' [47]. The addition of chitosan to PLGA scaffolds has been demonstrated to augment the number of interpore connections [27]. However, the incorporation of certain additives (e.g., plant extracts) has been observed to impede microchannels, thereby reducing overall connectivity [27].

6.5.2 Effects of processing parameters

In foamed cellulose acetate, an increase in pressure to approximately 250 bar has been observed to result in a reduction of the average pore size from 80 to around 20 μm, accompanied by a more uniform distribution [48]. In contrast, for cellulose aerogels, moderate pressures (~7.39 MPa) during supercritical drying are sufficient to preserve pore morphology while preventing collapse.

It has been demonstrated that foaming cellulose acetate at elevated temperatures (215–245°C) has a propensity to increase pore size [48]. However, for the supercritical drying of aerogels, lower temperatures (e.g., 31.1 or 60°C) are preferable in order to maintain structural integrity. In the case of cellulose acetate, saturation times between 180 and 480 minutes are employed to ensure a homogeneous pore structure [48]. In the process of drying starch gels (which are chemically similar to cellulose), it was determined that a 3-hour $scCO_2$ flow was effective [46].

In the domain of composite foams, the influence of additives on the characteristics of pores is a subject of significant interest. For instance, the incorporation of chitosan into PLGA has been observed to result in a reduction in pore size, while concurrently enhancing interconnectivity [27]. Conversely, the introduction of bioactive extracts (e.g., olive leaf extract (OLE)) has been shown to obstruct smaller pathways, thereby reducing connections [27]. In the field of PCL foams, the utilization of compounds such as μCMC and nanocellulose has been demonstrated to enhance porosity and morphology [38].

6.6 Other interesting biodegradable polymers and blends

6.6.1 PVA (poly(vinyl alcohol))

Although direct foaming of PVA using $scCO_2$ is rarely described in the literature, it has been used as a supporting matrix in systems where PMMA (poly(methyl methacrylate)) microparticles are foamed within a PVA film [45]. In such systems, PMMA foaming has been observed to produce nanoporous features (0–1000 nm), with porosity and pore size being amenable to control via process parameters [45].

6.6.2 Starch-based systems

The process of starch foaming via $scCO_2$ drying results in the formation of aerogels, which exhibit porosity levels ranging from 61 to 76%. These aerogels demonstrate a high degree of interconnectivity and the presence of submicron pores, with a diameter of less than 1 μm, as previously reported in [46]. Fibril diameters of approximately 20 nm have been observed to be prevalent [46]. Typical $scCO_2$ conditions involve saturation at 120 bar and 60°C for a duration of 3 hours. It has been demonstrated that thermoplastic starch undergoes significant microstructural and rheological changes during processing [49].

6.7 Long-term stability and degradation of foamed polymers

The long-term stability and degradation behavior of foamed biodegradable polymers are crucial for their effectiveness in applications, such as biomedical scaffolds, environmental filters, and compostable packaging. The stability and degradation behavior of these polymers are influenced by polymer chemistry, foam morphology (e.g., pore size and open-cell content), and environmental conditions, such as humidity, temperature, and microbial activity.

6.7.1 Structural integrity over time

Foamed PLA and PLGA scaffolds generally maintain structural integrity over short to medium periods (1–3 months), especially under dry or physiological conditions [24, 26]. However, hydrolysis of ester bonds in humid environments gradually reduces mechanical strength and pore wall thickness. For instance, PLGA foams stored at 37°C in a PBS solution undergo mass loss over time, with significant degradation commencing after 6–8 weeks [36].

PCL foams are known for their slow degradation rates. Under physiological conditions (37°C, PBS), structural integrity can be preserved for several months. Kosowska et al. [38] reported that PCL-based foams retained over 80% of their initial compressive strength after 8 weeks of immersion, particularly when reinforced with hydroxyapatite (HA).

PBS-based foams degrade more rapidly when exposed to microbial activity. While PLA/PBS blends are mechanically stable initially, they show signs of crack formation and pore coalescence after ~12 weeks of prolonged composting under industrial conditions [25, 34]. In open-air or marine environments, however, degradation is significantly slower and may lead to microplastic-like fragmentation if the material is not fully mineralized.

6.7.2 Influence of pore structure on degradation

Highly porous structures degrade faster due to their increased surface area and water uptake. Open-cell foams tend to undergo accelerated hydrolytic degradation, especially in amorphous regions. In contrast, microcellular structures degrade more gradually, but provide longer-lasting mechanical support.

Additives and blends influence long-term behavior.

- Chitosan enhances biodegradation, but it may reduce mechanical resistance over time [27].

- Nanoparticles (e.g., HA and SPIONs) delay degradation and improve mechanical retention [24, 40].

- Plasticizers and surfactants (e.g., eugenol or polyethylene glycol (PEG)) can accelerate degradation by increasing water uptake and chain mobility [41].

6.7.3 Outlook and testing recommendations

Future studies should include:

- Long-term soaking tests (≥3 months) in physiological and composting environments.

- Repeated mechanical testing (compression, Dynamic Mechanical Analysis (DMA)) to assess structural fatigue.

- In situ monitoring (e.g., micro-CT, SEM at intervals) to track pore collapse or coalescence.

It is essential to understand degradation pathways in order to match the lifespan of foam to the application. This is particularly important for temporary implants, biodegradable packaging, and controlled-release systems.

6.8 Functional additives in advanced applications

Not only do additives in $scCO_2$-foamed biodegradable polymers influence pore morphology, they also enable the design of multifunctional materials tailored for biomedical, environmental, and packaging applications. Their functions extend beyond structural reinforcement to include bioactivity, responsiveness, and delivery capabilities.

6.8.1 Antimicrobial and antioxidant activity

Natural bioactive compounds, such as carvacrol and olive pruning extracts, can be successfully impregnated during $scCO_2$ foaming. This yields porous materials with antimicrobial or antioxidant properties [27, 40]. These materials are particularly promising for use in active packaging and wound dressings, where barrier and therapeutic effects are desired.

6.8.2 Bioactivity and osteointegration

Nanofillers such as HA and chitosan promote osteoconductivity and enhance cell attachment in tissue engineering scaffolds [27, 38]. Their presence also modulates degradation rates and improves pore interconnectivity, making them ideal for bone regeneration and drug-releasing implants.

6.8.3 Controlled drug release

Some additives serve as both structural modifiers and drug carriers. For instance, PLGA foams impregnated with polyphenols or antibiotics via $scCO_2$ exhibit

prolonged release profiles over weeks [36]. These systems enable monolithic delivery scaffolds to be fabricated without the need for post-processing.

6.8.4 Electrical conductivity

Incorporating conductive polymers such as PEDOT:PSS or PANI confers electrical conductivity while maintaining foam porosity [37, 42]. These scaffolds are suitable for neural or cardiac tissue engineering, where electroactive environments can enhance cellular responses.

6.8.5 Thermal and mechanical enhancement

Carbon-based fillers (e.g., carbon nanotubes and graphene oxide) and microcellulose fibrils can enhance mechanical strength and thermal stability, as well as providing electromagnetic shielding properties.

7. A comparative analysis of polymers and emerging trends from 2018 to the present day

A review of recent literature from 2018 to 2025 reveals clear advancements in the use of supercritical CO_2 ($scCO_2$) foaming for biodegradable polymers. This encompasses both refinements in processing techniques and a more profound comprehension of how formulation and process variables influence foam morphology.

7.1 Porosity trends

The utilization of $scCO_2$ foaming has been demonstrated to be a highly effective method for the production of polymeric foams, with the porosity, pore size, and connectivity of these foams being able to be tuned to meet the requirements of a range of applications. These applications include biomedical scaffolds and packaging materials [5]. **Table 2** has been optimized for visualization.

7.2 Processing parameters

In **Table 3**, it can be observed that the role of $scCO_2$ foaming parameters is broadly consistent across different polymers, even though each system may respond uniquely due to differences in crystallinity, viscosity, and gas solubility.

Parameter	Observations	References
Porosity	High porosity (>80%) achievable in PLA, PLGA, and PCL. Influenced by CO_2 affinity, temperature, and additives like HA.	[5, 40]
Pore Size	Range from nanometers to millimeters. Bimodal structures seen in PLA/PBS/PBAT, suitable for bone tissue integration.	[29]
Interconnectivity	Interconnected pores up to 96% in PCL and 98.2% in PLA/PBS blends. Affected by depressurization rate and pore-opening additives.	[39]

Table 2.
Porosity trend parameters.

Parameter	Effects	Examples/Notes	References
Pressure	Higher pressure usually reduces pore size (PLA, PLGA, PCL), but may increase in P(3HB-co-4HB).	High nucleation density with elevated pressure.	[30, 35]
Temperature	Higher temperatures increase pore size via enhanced diffusivity and lower viscosity, but must be controlled to avoid instability.	Critical for semicrystalline polymers like PCL.	[30, 39]
Saturation Time	Longer times lead to uniform nucleation and structure; short times cause inconsistency.	Key for homogeneous CO_2 diffusion.	[30]
Depressurization Rate	Slow rate improves interconnectivity and larger pores; rapid rate yields smaller, uniform pores but less connectivity.	Staged depressurization effective in PLA/PBS/PBAT.	[29, 30]

Table 3.
Processing parameter trends.

Modification Type	Details	References
Nanofillers as Nucleating Agents	nHA, MCF, nGO, and SPIONs lower energy barrier for foaming, increase cell density, and reduce pore size.	[38]
Blends for Tailored Properties	PLA/PBS blends achieve up to 98.2% interconnectivity. Other blends enhance foam structure.	[25]
Crystallinity and Rheological Control	PLA/TPU improves crystallization; PHA + chain extenders boost rheological control.	[35]
Hybrid Processing Techniques	$scCO_2$ with two-step depressurization or plasticizers enables bimodal pores, throat tuning, and advanced tissue engineering.	[29, 41]

Table 4.
Impact of nanofillers and polymer blends.

7.3 Impact of nanofillers and polymer blends

In **Table 4**, it is developed how the employment of nanofillers and polymer blends is evolving into a progressively sophisticated approach to address limitations in foamability, morphology, and functional performance.

8. Characterization techniques used

In addition to porosity, pore size, and interconnectivity, studies on supercritical CO_2 foaming of biodegradable polymers frequently incorporate a broad range of characterization techniques (**Table 5**). These are essential for understanding the microstructure, chemical composition, thermal and mechanical properties, and even biological performance of the materials. Below is an overview of commonly employed techniques, grouped by characterization objective.

8.1 Morphology and pore architecture

Scanning Electron Microscopy (SEM) is widely used to investigate the surface morphology and cellular structure of polymer foams [9, 27, 38, 42, 43]. It provides

Characterization Category	Common Techniques	Purpose/Measurement
Morphological Structure	SEM, μCT, Optical Microscopy	Pore size, shape, interconnectivity
Chemical Composition	FTIR, XRD	Functional groups, crystallinity
Porosity and Surface Area	BET, MIP, Liquid Displacement	Total porosity, surface area, open-cell rate
Thermal Properties	DSC, TGA	Tg, Tm, thermal stability
Mechanical Properties	Tensile, Compression, DMA, Rheology	Strength, elastic modulus, viscoelasticity
Electrical/Biological	Conductivity, Cell Assays	Electroactivity, biocompatibility
Image Processing	ImageJ	Quantification from SEM/μCT images

Table 5.
Techniques used for characterization.

high-resolution imaging to assess pore size and distribution, cell wall thickness, structural uniformity, and the presence of defects or inclusions.

Transmission Electron Microscopy (TEM) is ideal for studying nanostructures and internal phase morphology, especially in multicomponent systems, such as polymer blends and block copolymers [50]. It offers atomic to nanometer-scale resolution by transmitting electrons through ultrathin samples.

Optical Microscopy is used for general observation of foam structure and cell formation, particularly where high magnification is not required [51].

X-ray Micro-Computed Tomography (μCT/Nano-CT) is a non-destructive 3D (three-dimensional) imaging technique that provides insights into internal structure, pore architecture, and interconnectivity [31]. Nano-CT enables higher resolution (down to ~50 nm voxel size), allowing quantification of porosity, surface area, and tortuosity [52].

8.2 Chemical structure and crystallinity

Fourier Transform Infrared Spectroscopy (FTIR) identifies functional groups, additives, and contaminants through characteristic infrared (IR) absorption bands. It provides a molecular fingerprint of the sample based on vibrational transitions.

X-ray Diffraction (XRD) is used to analyze the crystalline structure and degree of crystallinity of polymer materials. It is particularly useful in evaluating structural changes induced by foaming or by the addition of fillers [53].

8.3 Porosity and surface area analysis

Nitrogen (N_2) Physisorption/Brunauer-Emmett-Teller (BET)/Barrett-Joyner-Halenda (BJH) Methods are used to measure specific surface area (BET method) and pore size distribution (BJH method), particularly in the mesoporous range [54, 55].

Mercury Intrusion Porosimetry (MIP) characterizes pore volume, porosity, and pore size distribution by intruding mercury under increasing pressures. Larger pores fill at lower pressure; pore diameter is calculated via the Washburn equation [36].

Liquid Displacement/Archimedes' Principle determines open porosity and bulk density by measuring the displaced volume of a non-reactive liquid and comparing dry, wet, and submerged sample weights.

8.4 Surface and nanoscale properties

Atomic Force Microscopy (AFM) provides true 3D topographical mapping at nanometer resolution and can measure roughness, layer thickness, and domain size. It also offers qualitative mapping of mechanical properties, such as stiffness and adhesion.

8.5 Thermal stability and transitions

Differential Scanning Calorimetry (DSC) assesses thermal transitions like the glass transition temperature (Tg), melting point (Tm), and crystallization behavior, supporting material identification and processing optimization.

Thermogravimetric Analysis (TGA) evaluates thermal stability and compositional changes by measuring sample mass loss as a function of temperature or time. It helps determine filler content, moisture levels, and degradation profiles.

8.6 Mechanical properties

Tensile Testing measures the tensile strength, elastic modulus, and elongation at break by applying uniaxial tension to the material. Compression Testing is used to evaluate compressive strength and elastic modulus, providing data on how a material behaves under crushing or compressive forces. Shear Testing assesses a material's resistance to sliding deformation, especially useful for adhesives, composites, and soft materials. Dynamic Mechanical Analysis (DMA) characterizes viscoelastic behavior under oscillatory stress, providing data on storage modulus, loss modulus, and Tg across temperature or frequency sweeps. Rheology assesses flow behavior and deformation under different shear rates, temperatures, and time scales. It is crucial for processing studies and optimizing the viscoelastic performance of polymer melts or gels.

8.7 Functional and biological performance

For conductive polymer composites, techniques, such as 2-point/4-point probes or impedance spectroscopy, are used to determine electrical resistivity and conductivity. Cellular Assays (WST-1 (Water-soluble tetrazolium salt 1), Fluorostaining, Alkaline phosphatase (ALP)). These methods assess biocompatibility and cell behavior on scaffolds: WST-1: Measures metabolic activity as a proxy for cell viability. Fluorostaining: Uses fluorescent dyes for imaging cell attachment and morphology. ALP Assay: Evaluates osteogenic differentiation via alkaline phosphatase activity, a marker of early stage osteoblast function. Agitation/Cohesiveness Testing: Measures a material's internal cohesion and resistance to breakage during agitation. Techniques include powder flow analysis and unconfined compressive strength tests.

8.8 Image analysis tools

ImageJ is an open-source tool extensively used for quantitative analysis of micrographs from SEM or μCT. It allows measurements of cell size, pore density, and structural features through calibration, binarization, and segmentation.

9. Current challenges and future research directions

Despite considerable advances in the field of $scCO_2$ foaming of biodegradable polymers, several critical challenges remain to be addressed in order to fully exploit the potential of this technique, particularly with regard to biomedical and environmental applications.

A primary concern is the precise control and reproducibility of pore interconnectivity, which is vital for tissue engineering where nutrient diffusion and cell migration are essential [30]. Despite the noteworthy levels of interconnectivity that have been documented in PCL and PLA/PBS systems, the attainment of uniform, large-scale homogeneity continues to elude researchers. The formation of dense, non-porous surface layers continues to limit the functionality of the resulting foams in practical applications [30].

The intricate interplay of thermodynamic and kinetic phenomena inherent in the process of $scCO_2$ foaming introduces significant challenges to the accurate prediction and control of material morphology [2]. These challenges are further compounded in polymer blends and nanocomposites, where the behaviors of components and the interactions between CO_2 and polymers can be challenging to model and replicate.

In terms of scalability, $scCO_2$ foaming offers significant environmental and technical advantages; however, its industrial application is currently limited by several key challenges. These include the high capital investment required for high-pressure systems, the predominance of batch processes, and the need to customize parameters for each polymer formulation.

Several practical strategies have been developed to address these limitations. For instance, CO_2-assisted extrusion has emerged as a viable continuous method in which CO_2 is injected directly into the molten polymer. This allows for higher throughput and process automation [6]. Hybrid methods combining $scCO_2$ foaming with techniques, such as 3D printing, injection molding, or electrospinning, have also shown promise in modular upscaling, particularly in biomedical applications [56].

Successful pilot implementations include producing PLA/PBS foams for oil adsorption and compostable packaging [25], and manufacturing PCL-based scaffolds using $scCO_2$ that demonstrate clinical applicability [40]. Modular high-pressure systems offered by technology providers such as Thar Technologies and Separex facilitate gradual scale-up, enabling industry validation at different stages. Furthermore, integrating real-time pressure and temperature control systems enhances reproducibility and ensures compliance with regulations.

It is crucial that research efforts prioritize the development of more sophisticated processing methodologies. These methodologies should include multistage depressurization strategies that are precisely tailored to specific pressure-temperature profiles. This approach is expected to improve control over bimodal pore structures and their interconnectivity. Combining $scCO_2$ foaming with complementary fabrication methods such as electrospinning or additive manufacturing (e.g., 3D printing) shows promise in producing complex, hierarchical, and multifunctional materials [56].

Multifunctional Additive Design: Efforts must be concentrated on designing next-generation nucleating agents, plasticizers, and compatibilizers. These agents have a well-documented influence on pore structure, and it is now recognized that they can also impart additional functionalities, such as antibacterial activity, electrical conductivity, and enhanced biocompatibility. The effective dispersion of the additives and their compatibility with the polymer matrix will be pivotal to their success [42].

Modeling and Simulation Tools: Developing robust theoretical and computational models to simulate supercritical CO_2 foaming behavior across various polymer systems could significantly reduce the need for trial-and-error experimentation. This would accelerate material design and improve the scalability and predictability of foam properties.

Industrial Scalability and Sustainability: The transition from laboratory-scale to industrial-scale foaming presents a dual challenge, both technical and environmental in nature. The efficient recovery and reuse of carbon dioxide, in addition to process optimization for energy and material sustainability, is imperative for the large-scale manufacturing of $scCO_2$ foaming to be considered viable. Ultimately, the commercialization of $scCO_2$ foaming depends on selecting materials aligned with market needs, retrofitting existing lines for CO_2 use, and forming partnerships with end users in medical, packaging, or filtration sectors. The convergence of sustainable materials and scalable clean technology places $scCO_2$ foaming in a favorable position for broader industrial adoption.

Acknowledgements

We gratefully acknowledge the Spanish Ministry of Science and Innovation (Project PID2020-116229RB-I00) for financial support.

Conflict of interest

The authors declare no conflict of interest.

Author details

Ignacio García-Casas*, Diego Valor, Ludisbel León-Marcos, Antonio Montes and Clara Pereyra
Department of Chemical Engineering and Food Technology, Faculty of Sciences, University of Cadiz, International Excellence Agrifood Campus (CeiA3), Wine and Agrifood Research Institute (IVAGRO), Spain

*Address all correspondence to: ignacio.casas@uca.es

References

[1] Gonçalves LFFF, Reis RL, Fernandes EM. Forefront research of foaming strategies on biodegradable polymers and their composites by thermal or melt-based processing technologies: Advances and perspectives. Polymers. 2024;**16**

[2] Zhou Y, Tian Y, Peng X. Applications and challenges of supercritical foaming technology. Polymers. 2023;**15**

[3] Tapia-Blácido DR, Aguilar GJ, de Andrade MT, Rodrigues-Júnior MF, Guareschi-Martins FC. Trends and challenges of starch-based foams for use as food packaging and food container. Trends in Food Science and Technology. 2022;**119**:257-271

[4] Kemmere M, F, Meyer T. Supercritical Carbon Dioxide. In: Polymer Reaction Engineering. Supercritical Carbon Dioxide: In Polymer Reaction Engineering. Wiley-VCH Verlag GmbH & Co. KGaA; 2005. DOI: 10.1002/3527606726

[5] Liao X, Zhang H, He T. Preparation of porous biodegradable polymer and its nanocomposites by supercritical CO 2 foaming for tissue engineering. Journal of Nanomaterials. 2012;**2012**

[6] Sauceau M, Fages J, Common A, Nikitine C, Rodier E. New challenges in polymer foaming: A review of extrusion processes assisted by supercritical carbon dioxide. Progress in Polymer Science. 2011;**36**(6):749-766

[7] Alavi S, Rizvi SSH. Strategies for enhancing expansion in starch-based microcellular foams produced by supercritical fluid extrusion. International Journal of Food Properties. 2005;**8**(1):23-34

[8] Kazarian SG. Polymer processing with supercritical fluids. Polymer Science. 2000;**42**:78-101

[9] Villamil, Jiménez JA, Le Moigne N, Bénézet JC, Sauceau M, Sescousse R, Fages J. Foaming of PLA composites by supercritical fluid-assisted processes: A review. Molecules. 2020;**25**

[10] Jin FL, Zhao M, Park M, Park SJ. Recent trends of foaming in polymer processing: A review. Polymers. 2019;**11**

[11] Chen Z, Yin X, Chen H, Fu X, Sun Y, Chen Q, et al. Mechanical, crystallization, rheological, and supercritical CO2 foaming properties of polybutylene succinate nanocomposites: Impact of carbon nanofiber content. Polymers (Basel). 2024;**16**(1)

[12] Leja K, Lewandowicz G. Polymer biodegradation and biodegradable polymers - a review. Polish Journal of Environmental Studies. 2010;**19**(2):255-266

[13] Kim S, Chung H. Biodegradable polymers: From synthesis methods to applications of lignin-graft-polyester. Green Chemistry. 2024;**10774-803**

[14] Zhang C, Sun Z, Yang X, Guoyan Duan MW, Qiao Y. Effect of thermoplastic starch content on the properties of poly(butylene adipate-co-terephthalate) (PBAT) composites. Bioresources.cnr.ncsu.edu. 2025;**20**(2):3910-3922

[15] Cardea S, De MI. Cellulose acetate and supercritical carbon dioxide: Membranes, nanoparticles, microparticles and nanostructured filaments. Polymers (Basel). 2020;**12**(1)

[16] Chang HK, Chen PY. Synthesis of silica-based scaffolds with high porosity and controllable microstructure by a sintering-free sol–gel/freeze-casting hybrid method under mild conditions. Journal of Materials Research and Technology. 2020;**9**(6):16167-16178

[17] Haugen HJ, Monjo M, Rubert M, Verket A, Lyngstadaas SP, Ellingsen JE, et al. Porous ceramic titanium dioxide scaffolds promote bone formation in rabbit peri-implant cortical defect model. Acta Biomaterialia. 2013;**9**(2):5390-5399

[18] Olah L, Filipczak K, Jaegermann ZJ, Czigány T. Synthesis, structural and mechanical properties of porous polymeric scaffolds for bone tissue regeneration based on neat poly(ε-caprolactone) and its composites with calcium carbonate. Polymers for Advanced Technologies. 2006;**17**(11-12):889-897

[19] Tejchman A, Znój A, Chlebanowska P, Frączek-Szczypta A, Majka M. Carbon fibers as a new type of scaffold for midbrain organoid development. International Journal of Molecular Sciences. 2020;**21**(17):1-14

[20] Ambre A, Katti KS, Katti D. Nanoclay based composite scaffolds for bone tissue engineering applications. Journal of Nanotechnology in Engineering and Medicine. 2010;**1**

[21] Lalwani G, Gopalan A, D'Agati M, Sankaran JS, Judex S, Qin Y-X, et al. Porous three-dimensional carbon nanotube scaffolds for tissue engineering. Journal of Biomedical Materials Research. Part A. 2015;**103**(10):3212-3225

[22] Chen X, Feng JJ, Bertelo CA. Plasticization effects on bubble growth during polymer foaming. Polymer Engineering and Science. 2006;**46**(1):97-107

[23] Liu S, de Beer S, Batenburg KM, Gojzewski H, Duvigneau J, Vancso GJ. Designer Core–Shell nanoparticles as polymer foam cell nucleating agents: The impact of molecularly engineered interfaces. ACS Applied Materials and Interfaces. 2021;**13**(14):17034-17045

[24] Wang J, Zhang Y, Sun J, Jiao Z. Controllable fabrication of multi-modal porous PLGA scaffolds with different sizes of SPIONs using supercritical CO2 foaming. Journal of Applied Polymer Science. 2022;**139**(23)

[25] Li B, Zhao G, Wang G, Zhang L, Gong J, Shi Z. Biodegradable PLA/PBS open-cell foam fabricated by supercritical CO2 foaming for selective oil-adsorption. Separation and Purification Technology. 2021;**257**:117949

[26] Tayton E, Purcell M, Aarvold A, Smith JO, Kalra S, Briscoe A, et al. Supercritical CO2 fluid-foaming of polymers to increase porosity: A method to improve the mechanical and biocompatibility characteristics for use as a potential alternative to allografts in impaction bone grafting? Acta Biomaterialia. 2012;**8**(5):1918-1927

[27] García-Casas I, Valor D, Elayoubi H, Montes A, Pereyra C. Morphological 3D analysis of PLGA/chitosan blend polymer scaffolds and their impregnation with olive pruning residues via supercritical CO2. Polymers (Basel). 2024;**16**(11)

[28] Oluwabunmi K, D'Souza NA, Zhao W, Choi TY, Theyson T. Compostable, fully biobased foams using PLA and micro cellulose for zero energy buildings. Scientific Reports. 2020;**10**(1)

[29] Salerno A, Di Maio E, Iannace S, Netti PA. Solid-state supercritical CO2 foaming of PCL and PCL-HA nano-composite: Effect of composition,

thermal history and foaming process on foam pore structure. Journal of Supercritical Fluids. 2011;**58**(1):158-167

[30] Bhamidipati M, Scurto AM, Detamore MS. The future of carbon dioxide for polymer processing in tissue engineering. Tissue Engineering - Part B: Reviews. 2013;**19**:221-232

[31] Collins NJ, Bridson RH, Leeke GA, Grover LM. Particle seeding enhances interconnectivity in polymeric scaffolds foamed using supercritical CO2. Acta Biomaterialia. 2010;**6**(3):1055-1060

[32] Léonard A, Calberg C, Kerckhofs G, et al. Characterization of the porous structure of biodegradable scaffolds obtained with supercritical CO2 as foaming agent. Journal of Porous Materials. 2008;**15**:397-403

[33] Baldino L, Cardea S. Generation of biocompatible PCL foams by supercritical foaming. Chemical Engineering Transactions. 2020;**79**:241-246

[34] Chen PH, Chen CW, Chan TH, Lin HY, Tuan KL, Su CS, et al. Foaming of bio-based PLA/PBS/PBAT ternary blends with added nanohydroxyapatite using supercritical CO2: Effect of operating strategies on cell structure. Molecules. 2025;**30**(9)

[35] Zhang T, Jang Y, Lee E, Shin S, Kang HJ. Supercritical CO2 foaming of poly(3-hydroxybutyrate-co-4-hydroxybutyrate). Polymers (Basel). 2022;**14**(10)

[36] Valor D, Montes A, Monteiro M, García-Casas I, Pereyra C, de la Ossa EM. Determining the optimal conditions for the production by supercritical CO2 of biodegradable PLGA foams for the controlled release of rutin as a medical treatment. Polymers (Basel). 2021;**13**(10)

[37] Montes A, Valor D, Penabad Y, Domínguez M, Pereyra C, de la Ossa EM. Formation of PLGA–PEDOT: PSS conductive scaffolds by supercritical foaming. Materials. 2023 Mar;**16**(6)

[38] Kosowska K, Krzysztoforski J, Henczka M. Foaming of PCL-based composites using scCO2: Structure and physical properties. Materials. 2022;**15**(3)

[39] Song C, Luo Y, Liu Y, Li S, Xi Z, Zhao L, et al. Fabrication of PCL scaffolds by supercritical CO2 foaming based on the combined effects of rheological and crystallization properties. Polymers (Basel). 2020;**12**(4)

[40] Satpayeva A, Rojas A, Tyrka M, Ksepko E, Galotto MJ, Zizovic I. Supercritical foaming and impregnation of Polycaprolactone and Polycaprolactone-hydroxyapatite composites with Carvacrol. PRO. 2022;**10**(3)

[41] Tsivintzelis I, Pavlidou E, Panayiotou C. Biodegradable polymer foams prepared with supercritical CO2–ethanol mixtures as blowing agents. Journal of Supercritical Fluids. 2007;**42**(2):265-272

[42] Montes A, Valor D, Delgado L, Pereyra C, de la Ossa EM. An attempt to optimize supercritical CO2 polyaniline-Polycaprolactone foaming processes to produce tissue engineering scaffolds. Polymers (Basel). 2022;**14**(3)

[43] Lima GMR, Mukherjee A, Picchioni F, Bose RK. Characterization of biodegradable polymers for porous structure: Further steps toward sustainable plastics. Polymers (Basel). 2024;**16**(8)

[44] Oluwabunmi KE, Zhao W, D'souza N. Carbon capture utilization for biopolymer foam manufacture: Thermal,

mechanical and acoustic performance of PCL/PHBV CO2 foams. Polymers (Basel). 2021;**13**(15)

[45] Borgmann LM, Johnsen S, Santos de Oliveira C, de Souza M, J e S, Li J, et al. Porous polymeric microparticles foamed with supercritical CO2 as scattering white pigments. Bioinspiration and Biomimetics. 2023;**18**(2)

[46] Baudron V, Gurikov P, Smirnova I, Whitehouse S. Porous starch materials via supercritical-and freeze-drying. Gels. 2019;**5**(1)

[47] Grzybek P, Jakubski Ł, Dudek G. Neat chitosan porous materials: A review of preparation, structure characterization and application. International Journal of Molecular Sciences. 2022;**23**

[48] Reverchon E, Cardea S. Production of controlled polymeric foams by supercritical CO_2. Journal of Supercritical Fluids. 2007;**40**(1):144-152

[49] Atiwesh G, Mikhael A, Parrish CC, Banoub J, Le TAT. Environmental impact of bioplastic use: A review. Heliyon. 2021;**7**(9)

[50] Jinnai H. Electron microscopy for polymer structures. Microscopy. 2022;**71**:I148-I164

[51] Li W, Wei F, Xiong C, Ouyang J, Shao L, Dai M, et al. A novel supercritical CO2 foam system stabilized with a mixture of Zwitterionic surfactant and silica nanoparticles for enhanced oil recovery. Frontiers in Chemistry. 2019;**7**

[52] Scharf J, Chouchane M, Finegan DP, Lu B, Redquest C, Kim MC, et al. Bridging nano- and microscale X-ray tomography for battery research by leveraging artificial intelligence. Nature Nanotechnology. Nature Research. 2022;**17**:446-459

[53] Rinki K, Dutta PK, Hunt AJ, Clark JH, Macquarrie DJ. Preparation of chitosan based scaffolds using supercritical carbon dioxide. Macromolecular Symposia. 2009;**277**(1):36-42

[54] Long LY, Weng YX, Wang YZ. Cellulose aerogels: Synthesis, applications, and prospects. Polymers. 2018;**8**

[55] Rother G, Krukowski E, Wallacher D, Grimm N. Pore size effects on the sorption of supercritical CO2 in mesoporous CPG-10 silica. Journal of Physical Chemistry C. 2012;**116**(1):917-922

[56] Wang Z, Huang H, Wang Y, Zhou M, Zhai W. A review of the preparation of porous fibers and porous parts by a novel micro-extrusion foaming technique. Materials. 2024;**17**